

# Optically Induced Band Shifts in Infrared Spectra of Mixed Self-assembled Monolayers of Biphenyl Thiols

Jung F. Kang, Abraham Ulman,\* and Rainer Jordan

Department of Chemical Engineering, Chemistry and Materials Science, and NSF MRSEC for Polymers at Engineered Interfaces, Polytechnic University, Six Metrotech Center, Brooklyn, New York 11201

Dirk G. Kurth\*

Max-Planck-Institute of Colloids and Interfaces, Rudower Chaussee 5, D-12489 Berlin, Germany

Received April 7, 1999

Optically induced band shifts in reflection absorption infrared spectra (RAIR) of mixed self-assembled monolayers (SAMs) are reported. SAMs of 4-trifluoromethyl-4-mercaptobiphenyl dispersed in 4'-methyl-4-mercaptobiphenyl on gold exhibit significant shifts of the spectral envelope of the symmetric  $\text{CF}_3$  stretch and the  $b_{1u}$  skeletal mode. A linear relationship is observed between the band positions, the band intensity, and the surface  $\text{CF}_3$  group concentration. To rationalize the observed changes in band positions and shapes, a classical electromagnetic theory approach is used, providing an excellent agreement between theory and experiments. The simplified RAIR signature of 4'-trifluoromethyl-4-mercaptobiphenyl on gold is a unique example of the surface selection rule.

## Introduction

While self-assembled monolayers (SAMs) of alkane-thiolates on gold are one of the most thoroughly studied systems,<sup>1,2</sup> thiophenolate SAMs have only recently attracted attention.<sup>2–11</sup> This new class of SAMs offers the following advantages. First, biphenyl thiolates are rigid and planar molecules,<sup>12</sup> making these SAMs simple, yet ideal model systems to investigate surface phenomena. Second, chemical derivatization provides a simple means to change the electron density distribution in the molecule (e.g., its dipole moment). Third, 4-mercaptobiphenyl derivatives are readily available materials.<sup>13</sup> We have been

using alkane thiolate SAMs as model surfaces to study wetting,<sup>14</sup> adhesion,<sup>15</sup> and friction<sup>16</sup> and for surface-initiated ionic polymerization.<sup>17</sup>

Although many analytical techniques afford information on the elemental composition of surface layers, vibrational spectroscopy is unsurpassed in elucidating the nature, structure, and orientation of molecules at interfaces. The application of RAIR spectroscopy in surface analysis revealed many details of the molecular structure and will continue to play an important role in developing a comprehensive understanding of the nature of thin organic films.<sup>18</sup>

The chemical and structural analysis of RAIR spectra often relies on comparison with bulk spectra. Significant changes of the intensity contour of RAIR spectra compared to transmission spectra occur as a function of the refractive index of the material and the substrate as well as the orientation and packing of the molecules in the film.<sup>19</sup> To distinguish the optical, chemical, and structural effects, a theory approach is necessary. The RAIR experiment can be described by the interaction of a light beam with a smooth reflective surface. The theory which relates the macroscopic variables of the experiment with the incident and reflected electric fields at the interface is based on the boundary value solutions of Maxwell's equation for stratified media with uniform dielectric functions.<sup>20</sup> The simplest case involves an isotropic adsorbate layer identi-

\* Authors to whom correspondence may be addressed. For A. Ulman: Tel.: (718)260-3119. Fax: (718)260-3125. E-mail: aulman@duke.poly.edu. For D. G. Kurth: E-mail: kurth@MPIKG-GOLM.MPG.DE FAX: 49(0)331 567 9202.

(1) Ulman, A. *An Introduction to Ultrathin Organic Films*; Academic Press: Boston, 1991.

(2) Ulman, A. *Chem. Rev.* **1996**, *96*, 1533.

(3) Sabatani, E.; Cohen-Boulakia, J.; Bruening, M.; Rubinstein, I. *Langmuir* **1993**, *9*, 2974.

(4) Dhirani, A.-A.; Zehner, R. W.; Hsung, R. P.; Guyot-Sionnest, P.; Sita, L. R. *J. Am. Chem. Soc.* **1996**, *118*, 3319.

(5) Hsung, R. P.; Babcock, J. R.; Chidsey, C. E. D.; Sita, L. R. *Tetrahedron Lett.* **1995**, *36*, 4525.

(6) Hsung, R.; Chidsey, C. E. D.; Sita, L. R. *Organometallics* **1995**, *14*, 4808.

(7) Zehner, R. W.; Sita, L. R. *Langmuir* **1997**, *13*, 2973.

(8) Akiyama, T.; Imahori, H.; Ajawakom, A.; Sakata, Y. *Chem. Lett.* **1996**, 907.

(9) Tour, J. M.; Jones, L.; Pearson, D. L.; Lamba, J. J. S.; Burgin, Y. P.; Whitesides, G. M.; Allara, D. L.; Parikh, A. N.; Atre, S. *J. Am. Chem. Soc.* **1995**, *117*, 9529.

(10) Sachs, S. B.; Dudek, S. P.; Chidsey, C. E. D. *J. Am. Chem. Soc.* **1997**, *119*, 10563.

(11) Tao, Y.-T.; Wu, C.-C.; Eu, J.-Y.; Lin, W.-L.; Wu, K.-C.; Chen, C.-H. *Langmuir* **1997**, *13*, 4018.

(12) von Laue, L.; Ermark, F.; Götzhäuser, A.; Haeberlen, U.; Häcker, U. *J. Phys. Condens. Matter* **1996**, *8*, 3977.

(13) (a) Kang, J. F.; Jordan, R.; Ulman, A. *Langmuir* **1998**, *14*, 3983.

(b) Kang, J. F.; Liao, S.; Jordan, R.; Ulman, A. *J. Am. Chem. Soc.* **1998**, *120*, 9662. (c) Kang, J. F.; Ulman, A.; Liao, S.; Jordan, R. *Langmuir* **1999**, *15*, 2095. (d) Kang, J. F.; Ulman, A.; Liao, S.; Jordan, R. Submitted for publication in *J. Am. Chem. Soc.*

(14) Ulman, A.; Evans, S. D.; Shnidman, Y.; Sharma, R.; Eilers, J. E.; Chang, J. C. *J. Am. Chem. Soc.* **1991**, *113*, 1499.

(15) Kim, S.; Choi, G. Y.; Ulman, A.; Fleischer, C. *Langmuir* **1997**, *13*, 6850.

(16) Berman, A.; Steinberg, S.; Campbell, S.; Ulman, A.; Israelachvili, J. *J. Tribology* **1998**, in press.

(17) Jordan, R.; Ulman, A. *J. Am. Chem. Soc.* **1998**, *120*, 243.

(18) For studies on SAMs, see: Bishop, A. R.; Nuzzo, R. G. *Curr. Opin. Colloid Interface Sci.* **1996**, *1*, 127. For adsorbates on single-crystal metal surfaces, see: Hoffman, F. M. *Surf. Sci. Rep.* **1983**, *3*, 107.

(19) (a) Kurth, D. G.; Bein, T. *Langmuir* **1995**, *11*, 578. (b) Allara, D. L.; Baca, A.; Pryde, C. A. *Macromolecules* **1978**, *11*, 1215.

(20) Born, M. *Optik*; Springer: Berlin, 1932.

cal to a known bulk material on an ideally flat surface. The orientation of adsorbates, that is, the first moment of the orientation distribution, can be calculated from RAIR spectra because of the anisotropy of the interfacial wave field. The interference of the incident and reflected wave fields at grazing angles on a conducting substrate results in an enhanced electric field normal to the surface. Therefore, the intensity of a vibrational mode is, in general, given by the square of the scalar product of the electric field and the projection of the transition dipole moment on the surface normal. This is referred to as surface selection rules.<sup>21</sup> If the optical functions of the substrate and the adsorbate as well as the adsorbate layer thickness are available, it is, in principle, possible to compute the RAIR intensities as a function of orientation.<sup>22</sup> A more complicated situation arises when the adsorbate is anisotropic but otherwise identical to the bulk material. In this case, the refractive index should be formulated as an optical tensor.<sup>23</sup> Another problem in interpretation can be caused by surface roughness.<sup>24</sup> If adsorption significantly renders the force constants, normal modes, and charge distribution relative to the bulk material, it is impossible to make simple interpretations from a comparison of bulk and RAIR spectra.

In this account, we present a comprehensive analysis of RAIR spectra of 4'-trifluoromethyl-4-mercaptobiphenyl (**1**) and 4'-methyl-4-mercaptobiphenyl (**2**) mixed SAMs on gold. We report the first observation of optically induced band shifts in mixed SAMs. To rationalize the observed changes in band positions and shapes, a classical electromagnetic theory approach is used, providing excellent agreement between theory and experiments.

### Experimental Section

**Substrates.** Gold substrates were prepared by evaporating gold on glass slides (Fisher), without any adhesion layer, according to a procedure published elsewhere.<sup>25</sup>

**SAM Preparation.** SAMs and mixed SAMs of **1** and **2**<sup>13</sup> were prepared by adsorption from 10  $\mu$ M solutions in ethanol (for mixed SAMs the total concentration was 10  $\mu$ M). The thickness of all monolayers as estimated by ellipsometry was  $13 \pm 1$  Å, with almost no scattering of ellipsometric values throughout the sample. Advancing contact angles of water on all SAMs and mixed SAMs were essentially the same,  $85 \pm 1^\circ$ . Advancing methylene iodide (CH<sub>2</sub>I<sub>2</sub>) contact angles were  $60 \pm 1^\circ$  for **1** and  $42 \pm 1^\circ$  for **2**. Contact angle hysteresis was  $5^\circ$  in all cases, suggesting a uniform distribution of CF<sub>3</sub> and CH<sub>3</sub> groups. Monolayers stored under nitrogen, or in ethanol, for days showed no change in thickness and wettability.

**Fourier Transform Infrared Spectroscopy (FTIR).** Infrared spectra were recorded on a Nicolet 760 spectrometer with 1-cm<sup>-1</sup> resolution (2500 scans), using a SpectraTech 80° fixed grazing-angle attachment. RAIR spectra of **1** and **2** show a common band at 1003 cm<sup>-1</sup>, assigned to a  $b_{1u}$  fundamental mode,<sup>26</sup> of equal intensity. The integrated intensity of this band is the same for all spectra (within 5%), suggesting that mixed SAMs have essentially the same coverage and molecular orientation. The concentration of **1** in mixed monolayers was determined from the integrated intensity of the symmetric CF<sub>3</sub> (1327 cm<sup>-1</sup>)

mode. The errors were estimated to be smaller than  $\pm 5\%$  in the composition and less than  $\pm 0.0005$  a.u. in the absorbance.

**Scalar Optical Response Function.** The refractive index was determined by a method reported elsewhere.<sup>19</sup> For simplicity, the two bands at 1075 and 1340 cm<sup>-1</sup> were fitted by a Lorentzian profile using the expression

$$\hat{n}(\nu) = \sqrt{n_\infty^2 + \frac{f(\nu_0^2 - \nu^2) - i\Gamma\nu}{(\nu_0^2 - \nu^2)^2 + (\nu\Gamma)^2}} \quad (1)$$

where  $n_\infty$  is the refractive index far away from the absorption band (1.4 for **1** and **2**),  $f$  is the damping constant,  $\Gamma$  is the bandwidth,  $\nu_0$  is the peak position, and  $\nu$  stands for the wavenumber. On the basis of the IR spectrum of **1** in CCl<sub>4</sub>, the following parameters were found:  $\nu_0(b_{1u}) = 1072$  cm<sup>-1</sup>,  $f(b_{1u}) = 25\,000$  cm<sup>-2</sup>,  $\Gamma(b_{1u}) = 10$  cm<sup>-1</sup> and  $\nu_0(u+g) = 1327$ ,  $f(u+g) = 63\,000$  cm<sup>2</sup>,  $\Gamma(u+g) = 7$  cm<sup>-1</sup>. For a mixture of two noninteracting compounds, the refractive index is equal to the sum of the contributions due to each substance, that is,

$$\hat{n}(\nu) = \hat{n}_1(\nu)\chi + \hat{n}_2(\nu)(1 - \chi) \quad (2)$$

Here,  $\chi$  is the molar fraction and  $\hat{n}_1(\nu)$  and  $\hat{n}_2(\nu)$  are the refractive indices of compounds **1** and **2**. The refractive index of the underlying substrate was taken from the literature.<sup>27</sup>

**Model.** To compute the RAIR intensity, we employ a model of plane parallel layers with homogeneous, isotropic dielectric constants.<sup>28</sup> It can be shown that the boundary value solution of Maxwell's equation for the reflectance of a single film on a substrate can be reduced to

$$R_{0/1/2} = \frac{R_{0/1} + R_{1/2} + 2Re[r_{0/1}r_{1/2}e^{-2\hat{\nu}_1d_1}]}{1 + R_{0/1} + R_{1/2} + 2Re[r_{0/1}r_{1/2}e^{-2\hat{\nu}_1d_1}]} \quad (3)$$

$R$  is the reflectance,  $r$  is the reflection coefficient,  $Re$  indicates the real part of the expression in parentheses, and  $d_1$  is the film thickness. The reflection coefficients at each interface are given by the Fresnel equation:

$$r_{ij} = \frac{\hat{n}_j \cos[\phi_j] - \hat{n}_i \cos[\phi_i]}{\hat{n}_i \cos[\phi_j] + \hat{n}_j \cos[\phi_i]} \quad (4)$$

The angle of incidence in each medium is given by the Snell equation  $\hat{n}_i \sin[\phi_i] = \hat{n}_j \sin[\phi_j]$ . The reflectance,  $R_{ij}$ , equals the square modulus of the reflection coefficient. The phase factor  $\hat{\nu}_1$  of medium 1 is given by  $\hat{\nu}_1 = 2\pi\nu\hat{n}_1 \cos[\phi_1]$ . Care must be taken to compute the proper sign of the phase factor.<sup>29</sup> The RAIR absorbance is given by

$$A = -\text{Log}_{10} \left[ \frac{R_f}{R_s} \right] \quad (5)$$

where  $R_f$  is the reflectivity of the film-substrate interface and  $R_s$  is the reflectivity of the substrate (no film present). The free parameters are the film thickness (determined by ellipsometry) and the bandwidth (determined from RAIR spectra).

If the adsorbate molecules are oriented but otherwise identical to the bulk material, the intensities of each mode are scaled to the following condition:

$$A \propto |\bar{\mu} \cdot \bar{n}|^2 |\bar{E}|^2 \quad (6)$$

where  $\bar{n}$  is the surface normal,  $\bar{\mu}$  is the transition dipole moment, and  $\bar{E}$  is the electric field vector. The refractive index in the infrared is usually obtained from a randomly oriented bulk phase. As a result, alignment of the dipole moments of the adsorbate molecules gives an experimentally observed intensity for each mode of 3 times that for the calculated isotropic spectrum. This

(21) Pearce, H. A.; Sheppard, N. *Surf. Sci.* **1976**, *59*, 205.

(22) Allara, D. L.; Nuzzo, R. G. *Langmuir* **1985**, *1*, 52.

(23) Parikh, A. N.; Allara, D. L. *J. Chem. Phys.* **1992**, *96*, 927.

(24) Dignam, M. J.; Moskovits, M. *J. Chem. Soc., Faraday Trans. 2* **1973**, *1*, 65.

(25) The slides were baked at 300 °C in a vacuum overnight. A thickness of 1000 Å of gold was evaporated at a deposition rate of 1.5–2 Å/s at 300 °C and the samples were annealed at this temperature for 18 h. Imaging with atomic force microscopy (Digital Instruments Nanoscope III) revealed plateaus of up to 5000 Å diameter. Putnam, A.; Blackford, M. H.; Jerico, M. H.; Watanabe, M. O. *Surf. Sci.* **1989**, *217*, 276.

(26) Ferguson, E. E.; Hudson, R. L.; Nielsen, J. R.; Smith, D. C. *J. Chem. Phys.* **1953**, *21*, 1736.

(27) Palik, E. D. *Handbook of Optical Constants of Solids*; Academic Press: San Diego, CA, 1985.

(28) Greenler, R. *J. Chem. Phys.* **1966**, *44*, 310.

(29) Hansen, W. N. *J. Opt. Soc.* **1968**, *58*, 380.

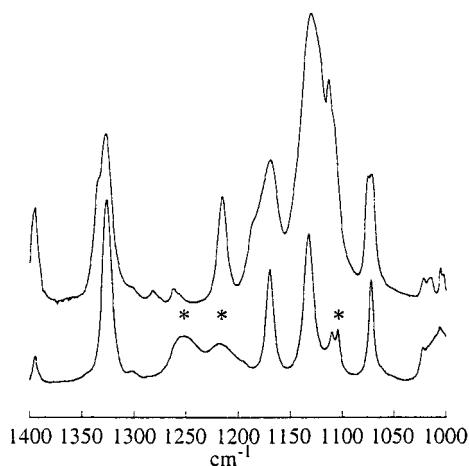


**Figure 1.** Comparison of the transmission infrared spectra of **1** in the solid (top, KBr pellet) and the liquid (bottom,  $\text{CCl}_4$ ) state. The relative intensities and the width of the bands react sensitively to the physical state of the material. The asterisk indicates bands of  $\text{CCl}_4$ .

approach has gained wide acceptance since it requires few approximations and has been shown previously to be quantitatively valid.<sup>30</sup>

## Results and Discussion

**Transmission Infrared Spectra and Mode Assignment.** The infrared spectrum of 4'-trifluoromethyl-4-mercaptobiphenyl (**1**) can be rationalized if the skeletal fundamental modes are assigned based on a model of symmetry  $D_{2h}$ , according to which the  $\text{CF}_3$  groups are assumed to be points, and to add to these the fundamental modes of the  $\text{CF}_3$  groups.<sup>26</sup> Compound **1** shows unusually strong bands in the mid infrared region. The band contours and the relative intensities react sensitively to the physical state of the material. The IR spectrum of **1** dissolved in a liquid shows narrow, resolved bands, whereas a solid dispersion of **1** shows broad bands (Figure 1). Because of the strong permanent dipole moment of the  $\text{CF}_3$  moiety and of the molecule as a whole due to the electron donor and acceptor properties of the SH and  $\text{CF}_3$  substituents, as well as possible  $\pi$ -stacking interactions of the aromatics, strong molecular interactions are expected. The random nature of such interactions is expected to increase the bandwidth through lifetime broadening, vibrational coupling, and other inhomogeneous broadening mechanisms. In dilute solution, molecular interactions are diminished by the surrounding solvent. The translational and rotational motions may fluctuate more rapidly, resulting in motional narrowing of the bands.<sup>31</sup> The relevant peak positions and assignments for compound **1** are summarized in Table 1.

**Reflection–Absorption IR Spectra.** SAM of **1**. The RAIR spectrum of a SAM of **1** shows two striking features (Figure 2). First, the intensity contour is dramatically simplified, and second, the band maxima are shifted to higher energy. On the basis of the discussion of the previous section, the transition dipole moments have the following directions (Table 1).<sup>32</sup>

The transition dipole moments of the antisymmetric  $\text{CF}_3$  stretching modes (1133 and 1170  $\text{cm}^{-1}$ ) are perpen-

**Table 1.** Peak Positions, Assignments, and Directions of the Transition Dipole Moments of the Most Prominent Infrared Bands of 4'-Trifluoromethyl-4-mercaptobiphenyl in  $\text{CCl}_4$  ( $x, y, z$  Form a Right-Hand System; the Molecular Axis Defines  $z$ )

position ( $\text{cm}^{-1}$ )	intensity	symmetry	direction of $\mu$	assignment
1072	vs	$b_{1u}$	$z$	fundamental skeletal mode
1133	vvs	$u + g$	$x, y$	asym $\text{CF}_3$
1170	vvs	$u + g$	$x, y$	asym $\text{CF}_3$
1327	vvs	$u + g$	$z$	sym $\text{CF}_3$

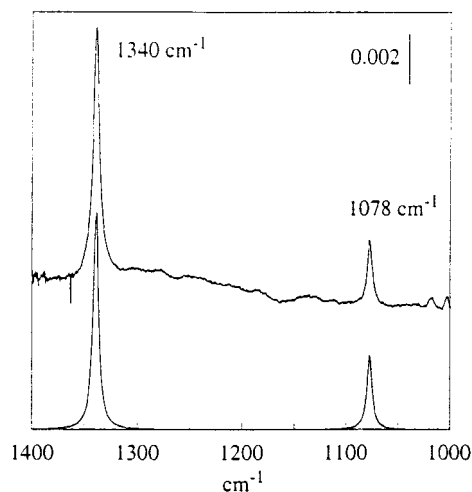


**Figure 2.** Uncorrected RAIR spectrum of **1** on gold (top, angle of incidence:  $80^\circ$ ). Because of the simplified signature of the RAIR spectrum, only the symmetric  $\text{CF}_3$  mode and the  $b_{1u}$  skeletal mode were computed assuming an upright orientation of **1** on the surface (bottom contours). On the basis of the absence of the antisymmetric  $\text{CF}_3$  stretching modes, it follows directly from the surface selection rules that **1** must be oriented in the direction of the surface normal. The spectra are offset for clarity.

dicular to the molecular axis and in and out of the plane defined by the aromatic rings ( $x, y$  direction). The complete absence of these two modes in the RAIR spectrum implies that the transition dipole moment of these modes must be oriented parallel to the surface. The transition dipole moment of the symmetric  $\text{CF}_3$  (1327  $\text{cm}^{-1}$ ) and the  $b_{1u}$  skeletal mode (1072  $\text{cm}^{-1}$ ) are in the direction of the molecular axis ( $z$  direction). The presence of these two modes (1072  $\text{cm}^{-1}$ ) implies that the transition dipole moments are oriented normal to the surface. The symmetric  $\text{CF}_3$  and the  $b_{1u}$  skeletal mode are orthogonal to the antisymmetric  $\text{CF}_3$  stretching modes. On the basis of the surface selection rule, there is only one possible explanation for the simplified signature of the RAIR spectrum: the molecules are almost exclusively oriented in the direction of the surface normal.<sup>33</sup> The bottom part of Figure 2 shows the calculated band intensities of the symmetric  $\text{CF}_3$  and the skeletal mode for a monolayer based on the assumption of an upright orientation. The relative and absolute computed intensities are in excellent agreement with the experimental values.

A comparison with the infrared transmission data (Table 1) reveals that the symmetric  $\text{CF}_3$  mode is shifted from 1327  $\text{cm}^{-1}$  (transmission) to 1340  $\text{cm}^{-1}$  (SAM) and the  $b_{1u}$  skeletal mode is shifted from 1072  $\text{cm}^{-1}$  (transmission) to 1078  $\text{cm}^{-1}$  (SAM), respectively. The computed peak

(30) Porter, M. D.; Bright, T. B.; Allara, D. L. *Anal. Chem.* **1986**, *58*, 2461.

(31) Steele, D.; Yarwood, J., Eds. *Spectroscopy and Relaxation of Molecular Liquids*; Elsevier: Amsterdam, 1991.

(32) Herzberg, G. *Molecular Spectra and Molecular Structure*; Krieger: Malabar, FL, 1992.

(33) This mode of orientation may require a  $180^\circ$  bond angle at the sulfur atom ( $sp$  hybridization). This is in agreement with our simulation results that the energy difference between  $sp$  and  $sp^3$  hybridization at the sulfur atom is small. See: Sellers, H.; Ulman, A.; Shnidman, Y.; Eilers, J. E. *J. Am. Chem. Soc.* **1993**, *115*, 9389.

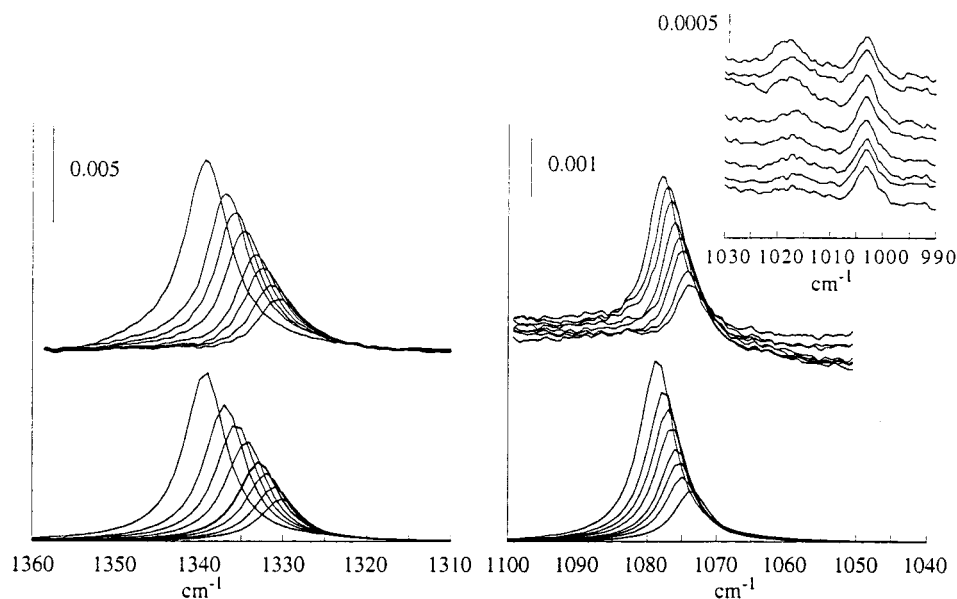


**Figure 3.** The experimental RAIIR bands of mixed monolayers of **1** and **2** (top) and the calculated band intensities of the  $b_{1u}$  skeletal and the symmetric  $\text{CF}_3$  stretching mode (bottom). The inset shows the skeletal  $b_{1u}$  and  $b_{3u}$  fundamental modes at 1003 and 1017  $\text{cm}^{-1}$ . The compositions of each monolayer are from bottom to top: 27, 34, 43, 51, 63, 72, 81, and 100% **1**. The bar indicates the intensity for the experimental and calculated spectra, respectively.

positions (1339 and 1078  $\text{cm}^{-1}$ ) are, again, in excellent agreement with the experimental values. An analysis of the origin of these peak shifts will be given in the next section.

Compared to the infrared spectra of **1** in the solid and the liquid state (Figure 1), the RAIIR spectrum (Figure 2) coincides best with the solution spectra in terms of the general band contours and relative intensities. The intermolecular interactions present in the solid seem to be absent in the monolayers. Intuitively, one would expect molecular interactions to be diminished in oriented monolayer assemblies. This is supported by the noteworthy observation that the bandwidth of the symmetric  $\text{CF}_3$  (7  $\text{cm}^{-1}$ ) and the  $b_{1u}$  skeletal mode (5  $\text{cm}^{-1}$ ) is smaller in the monolayer than in the liquid state (10 and 6  $\text{cm}^{-1}$ , respectively). Apparently, dissipative mechanisms operative on adsorbed species play only a minor role.<sup>34</sup> For this reason, the refractive index of the  $\nu_s(\text{CF}_3)$  and the  $b_{1u}$  skeletal mode was determined from the transmission IR spectrum of **1** in  $\text{CCl}_4$ .

**Mixed SAMs.** Figure 3 shows the RAIIR spectra (top) of the  $b_{1u}$  skeletal and the symmetric  $\text{CF}_3$  stretching mode of mixed monolayers of **1** and **2** as well as the computed band contours (bottom) for these modes. Compound **2** does not show interfering peaks in these regions. The composition of each monolayer is from bottom to top: 27, 34, 43, 51, 63, 72, 81, and 100% **1**. This is the first example of concentration-dependent peak shifts in RAIIR spectra of SAMs. The following factors influencing the peak positions of adsorbates have been identified in the literature: (a) the blue shift due to mechanical renormalization, (b) chemical effects due to surface bonding, and (c) lateral interactions between neighboring oscillators (vibrational coupling).<sup>35</sup> A change of force constants, normal modes, or charge distribution induced by (a) or (b) as a result of adsorption seems unlikely. One would expect this effect

to be operative at all coverages which is not observed. In addition, the  $b_{1u}$  fundamental mode at 1003  $\text{cm}^{-1}$ , common for both compounds **1** and **2**, remains constant in position and intensity for all concentrations (inset Figure 3).

Vibrational coupling effects (c) encompass both through-bond and through-space interactions of adjacent oscillators and cause a coverage-dependent frequency shift.<sup>36</sup> It can be shown that the vibrational coupling constants are a function of the energy separation of the modes under consideration. Since the vibrational frequencies for **1** and **2** are widely separated, the coupling constants are negligible. The  $\nu_s(\text{CF}_3)$  and the  $b_{1u}$  skeletal mode can be considered as isolated vibrations. As a result, mechanism (c) is of only minor importance. The model employed to compute the band contours does not take into account electronic or coupling effects. It considers the mixed monolayer as a thin film with an effective refractive index which is equal to the sum of the contributions due to each substance; the reflectance is computed from first electromagnetic principles (see Experimental Section for details). The excellent agreement of experimental and computed band contours suggests that the major effect is a purely optical one and that other mechanisms are of minor importance. It should be pointed out that we do not observe a concentration-dependent bandwidth or a change of relative intensities; on the contrary, the bandwidth and the peak intensity ratio ( $\nu_s(\text{CF}_3)/b_{1u}(\text{skeletal mode})$ ) remain constant ( $2.77 \pm 0.1$ ). This is another indication for the absence of coupling mechanisms.

The assumption of using an effective refractive index equal to the sum of the contributions due to each substance requires that the mixture behaves like an ideal solution (no change of density and absence of strong molecular interactions). This is in agreement with the observation made above that molecular interactions in mixed monolayers are diminished. Contributions from anisotropy in these films are also negligible. The agreement of theory

(34) Ueba, H. *Prog. Surf. Sci.* **1986**, *22*, 181.

(35) For a general introduction, see: Bradshaw, A. M.; Schweizer, E. In *Advances in Spectroscopy. Spectroscopy of Surfaces*; Hester, R. E., Clark, R. J. H., Eds.; Wiley: New York, 1988; Vol. 16, pp 413–488 and references cited herein. The “self-image” shift causes a peak shift toward lower energy and can be ruled out as a principle mechanism.

(36) Willis, R. F.; Lucas, A. A.; Mahan, G. D. *The Chemical Physics of Solid Surfaces and Heterogeneous Catalysis*; King, D. A., Woodruff, D. P., Eds.; Elsevier: Amsterdam, 1981; Vol. 2, pp 67–100.

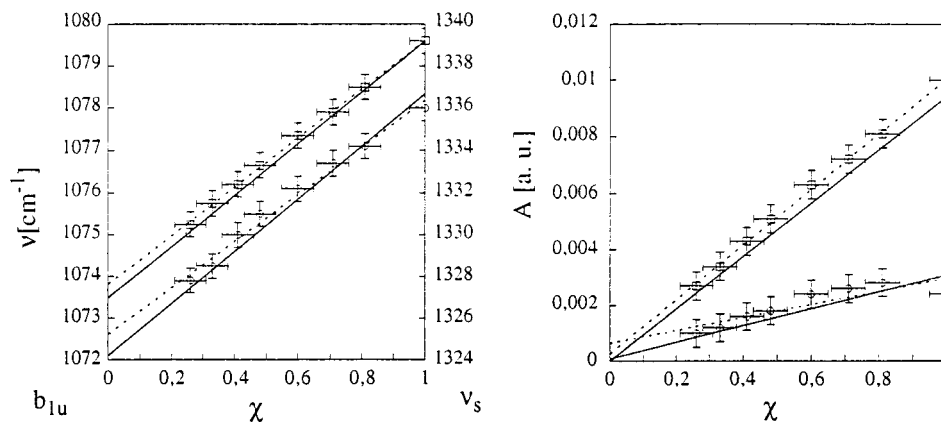


**Figure 4.** Experimental and calculated peak shifts and intensities of the  $\nu_s$   $\text{CF}_3$  (squares) and the  $b_{1u}$  skeletal (circles) modes in mixed SAMs of **1** and **2**. The solid lines are linear regressions of the computed values. The dotted curves are linear regressions of the experimental values.

and experiment with this simple model for the optical response function is indeed remarkable.

The peak shift can be understood as follows: Because of the standing wave field on a conducting substrate, the amount of radiation removed from the incident beam is governed by the reflectivity and absorptivity of the film–substrate interface. In a simplified analysis, the reflectance is attributed to the real part  $n(\nu)$ , while the absorptivity is connected with the imaginary  $k(\nu)$  of the complex refractive index,  $\hat{n}(\nu)$ . The strong anomalous dispersion of the modes under consideration results in an enhanced reflectivity (more light at the detector) at the low-energy side and a reduced reflectivity (less light at the detector) at the high-energy side of the band maxima,  $\nu_0$ . This results in an apparent shift of the band contour toward higher energy.<sup>37</sup>

Figure 4 shows the experimentally observed and computed band shifts (solid lines) and band intensities (peak value) of the two modes as a function of the  $\text{CF}_3$  concentration in the mixed SAM. It should be noted that the extrapolation of the intensity to zero coverage (dotted curve) for the symmetric  $\text{CF}_3$  mode passes through the origin. The extrapolation of the peak shifts to zero coverage (dotted line, 1327.6 and 1072.7  $\text{cm}^{-1}$ ) is equal to the peak positions of the liquid sample (1327 and 1072  $\text{cm}^{-1}$ ). These two findings indicate that, first, all molecules contribute equally to the intensity and, second, that domain formation in mixed SAMs can be ruled out.<sup>38</sup> Because of the less well-defined baseline in the region of the skeletal mode at 1070  $\text{cm}^{-1}$  (Figure 3), the intensity data have more scatter but they show the same trends. The solid curves in Figure 4 are linear regressions of the computed values; they are in excellent agreement with the experimental data both in terms of peak position and intensity. In as much as we were able to compute both the peak positions and peak intensities for the symmetric  $\text{CF}_3$  and the skeletal mode as a function of composition close to those observed

experimentally, our approach is in a sense validated by this simultaneous agreement.

### Conclusions

We present a unique example of the surface selection rules: 4'-trifluoromethyl-4-mercaptobiphenyl (**1**) forms self-assembled monolayers in which the molecules are oriented in the direction of the surface normal. This result is directly inferred from the complete absence of the antisymmetric modes of the  $\text{CF}_3$  group in the RAIR spectrum of **1**. The transition dipole moments of these modes are perpendicular to the molecular axis.

For the first time, we report optically induced peak shifts in mixed self-assembled monolayers of 4'-trifluoromethyl-4-mercaptobiphenyl (**1**) and 4'-methyl-4-mercaptobiphenyl (**2**). We demonstrate that peak shifts are caused by optical effects as a result of the strong anomalous dispersion of the modes. To compute the reflectance of the thin film interface, the optical response function of mixed SAMs is approximated by an isotropic effective refractive index equal to the sum of contributions from each component. The simultaneous close agreement of calculated and experimentally observed peak positions and peak intensities as a function of composition validates our approach.

Our analysis shows that the orientation of the transition dipole moments remains the same in pure and mixed SAMs. From a comparison of transmission IR spectra and RAIR spectra, we infer that molecular interactions in SAMs, such as  $\pi$ -stacking or dipolar interactions, are diminished as one would expect for oriented monolayer assemblies.

**Acknowledgment.** D.G.K. is very grateful to Prof. H. Möhwald for valuable discussions and acknowledges the Max-Planck-Society for financial support. Support from the National Science Foundation through the MRSEC for Polymers at Engineered Interfaces and from the Lord Corporation is gratefully acknowledged. R.J. is thankful for the postdoctoral fellowship supported by the Deutsche Forschungsgemeinschaft.

LA9904051

(37) Greenler, R. G.; Rahm, R. R.; Schwartz, J. P. *J. Catal.* **1971**, *23*, 42.

(38) Patches of analyte with an approximate size of the employed wavelength would create coherent wave fronts; as a result, refraction and reflection occur as governed by the optical constants of the pure analyte. Such a sample would show a constant peak position independent of concentration.